Supporting Information

Bio-Inspired Bi-Anisotropic Magneto-Sensitive Elastomers with Excellent Multimodal Transformation

Jingyi Zhang[1], Yu Wang[1*], Huaxia Deng[1], Chunyu Zhao[1], Yanan Zhang[2], Haiyi Liang[2], Xinglong Gong[1*]

[1]*CAS Key Laboratory of Mechanical Behavior and Design of Materials, Department of Modern Mechanics, University of Science and Technology of China (USTC), Hefei 230027, P. R. China.*

[2]*IAT-Chungu Joint Laboratory for Additive Manufacturing, Institute of Advanced Technology, University of Science and Technology of China (USTC), Hefei 230027, P. R. China.*

**Corresponding author: wyu@ustc.edu.cn (Y. Wang), gongxl@ustc.edu.cn (X. Gong)*

Section S1: The magnetization constitutive of the anisotropic MSE sample.

As shown in figure 2d, the hysteresis loops of shape anisotropic MSE do not coincide when installed in different positions of the magnetic field. The susceptibility is greater when the longitudinal direction of the sample is horizontal to the direction of the external magnetic field. Therefore, when calculating the magnetization $\mathbf{M}$ of the RVE, the demagnetization field $\mathbf{H_D}$ is considered.

$$\mathbf{H_D} = -\mathbf{n} \cdot \mathbf{M} \tag{S1}$$

Where $\mathbf{n} = \begin{bmatrix} n_1 & 0 \\ 0 & n_2 \end{bmatrix}$ is demagnetization factor tensor.

The initial magnetic field intensity is $\mathbf{H_0}$

$$\mathbf{H_0} = \begin{bmatrix} \mathbf{H_0 cos\ \beta} \\ \mathbf{H_0 sin\ \beta} \end{bmatrix} \tag{S2}$$

β is the longitudinal axis of the beam to the direction of the magnetic field. $\beta = \frac{\pi}{2} - \theta - \alpha$. The internal magnetic intensity of the sample can be expressed as

$$\mathbf{H} = \mathbf{H_0} + \mathbf{H_D} \tag{S3}$$

According to magnetization theory, we have

$$\mathbf{M} = \boldsymbol{\chi}\mathbf{H} \tag{S4}$$

From Eq. **S1**, **S3** and **S4**, the relationship of $\mathbf{M}$ and $\mathbf{H_0}$ can be obtained

$$\mathbf{M} = \frac{\chi}{\mathbf{1}+\boldsymbol{\chi}\mathbf{n}}\mathbf{H_0} = \begin{bmatrix}\boldsymbol{\chi_1}\\ \boldsymbol{\chi_2}\end{bmatrix}\mathbf{H_0} \tag{S5}$$

Where $\chi_1 = \frac{\chi}{1+\chi n_1}$ and $\chi_2 = \frac{\chi}{1+\chi n_2}$.

Section S2

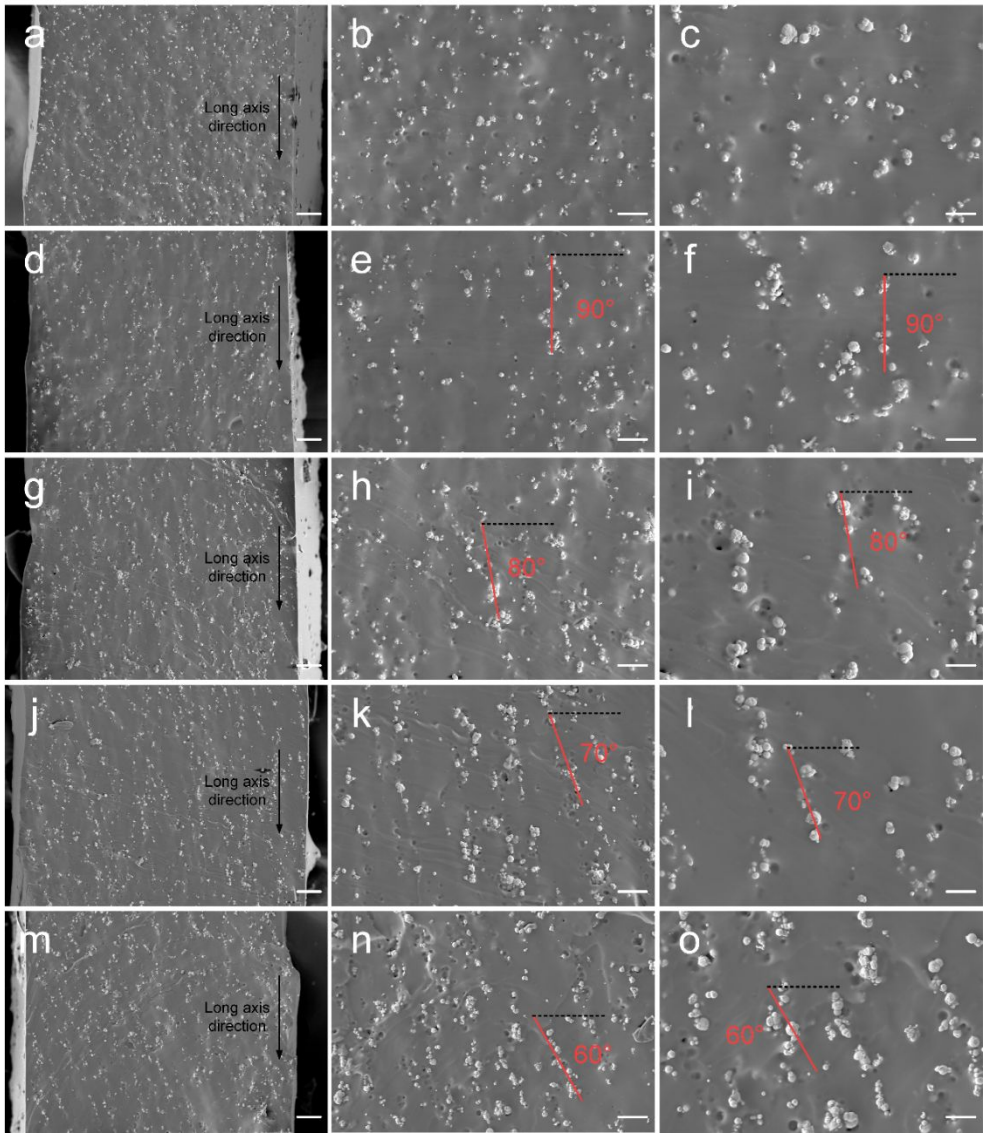

Figure S1 The SEMs of magneto-sensitive elastomers (MSEs) with 50 wt% carbonyl iron (CI) particles. The microstructure and long axis direction of material isotropic sample (a), material anisotropic 90° sample (d), material anisotropic 80° sample (g) and 70° sample (j) and 60° sample (m). Scale bar, 40 μm. (b-c) (e-f) (h-i) (k-l) (n-o) Local magnification of (a) (d) (g) (j) and (m). Scale bar, 20 μm and 10 μm.

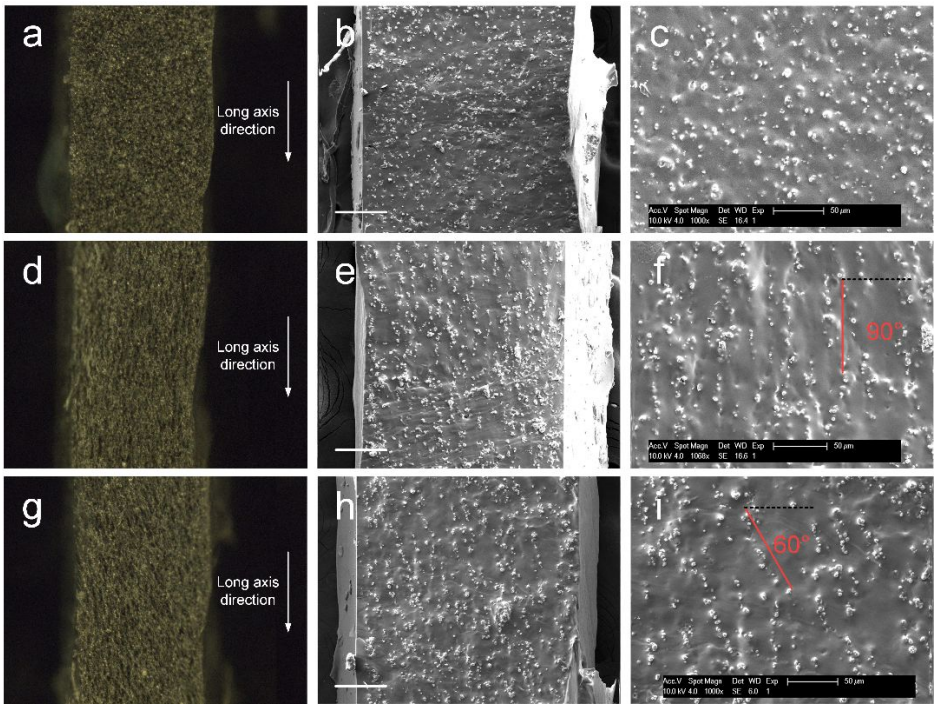

Figure S2 The cross section comparison of three samples. The optical micrographs, SEMs and enlarged SEMs of material isotropic sample (a-c), anisotropic 90° sample (d-f) and anisotropic 60° sample (g-i). Scale bar, 100 μm.

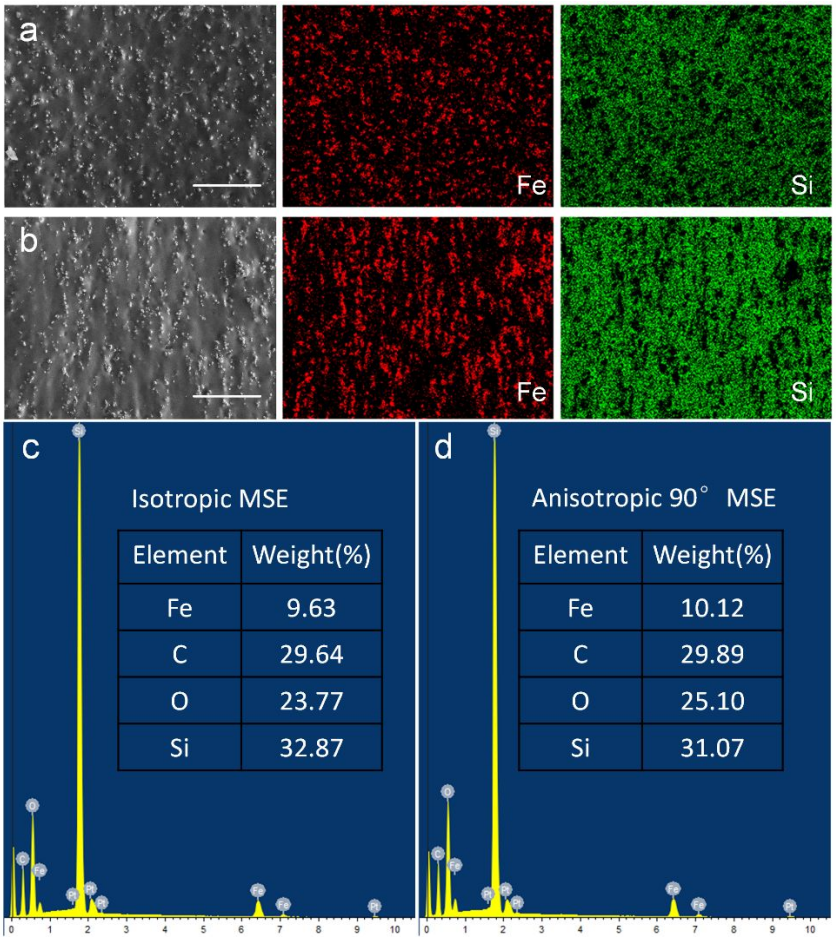

Figure S3 SEM images of material isotropic sample (a) and anisotropic 90° sample (b), and the related element EDS mapping of Fe and Si. (c-d) EDX diagram and elemental composition of two samples.

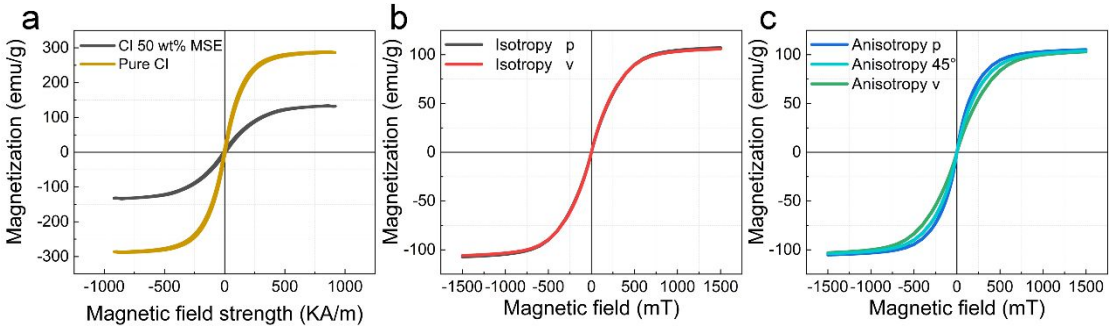

Figure S4 (a) The magnetization curves of pure CI and MSE. (b) The magnetization curves of disk material isotropic MSE when placed in a parallel and vertical magnetic field. (c) The magnetization curves of disk material anisotropic MSE when internal particle chain orientation is parallel, 45° and perpendicular to magnetic field direction.

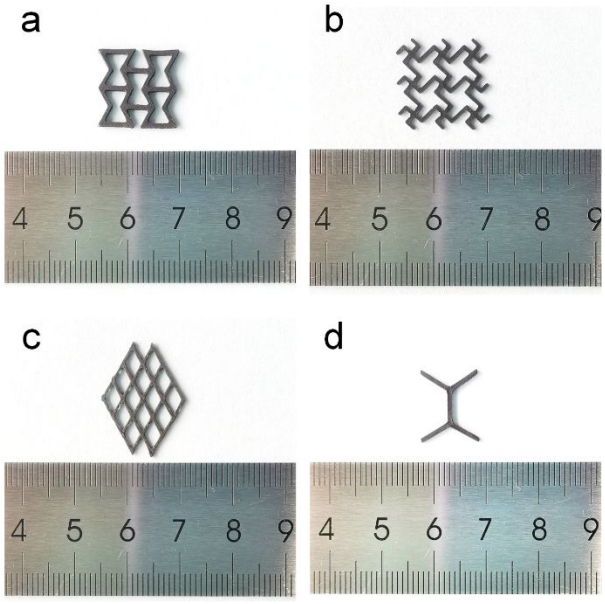

Figure S5 Various shape anisotropic MSEs with different architectures.

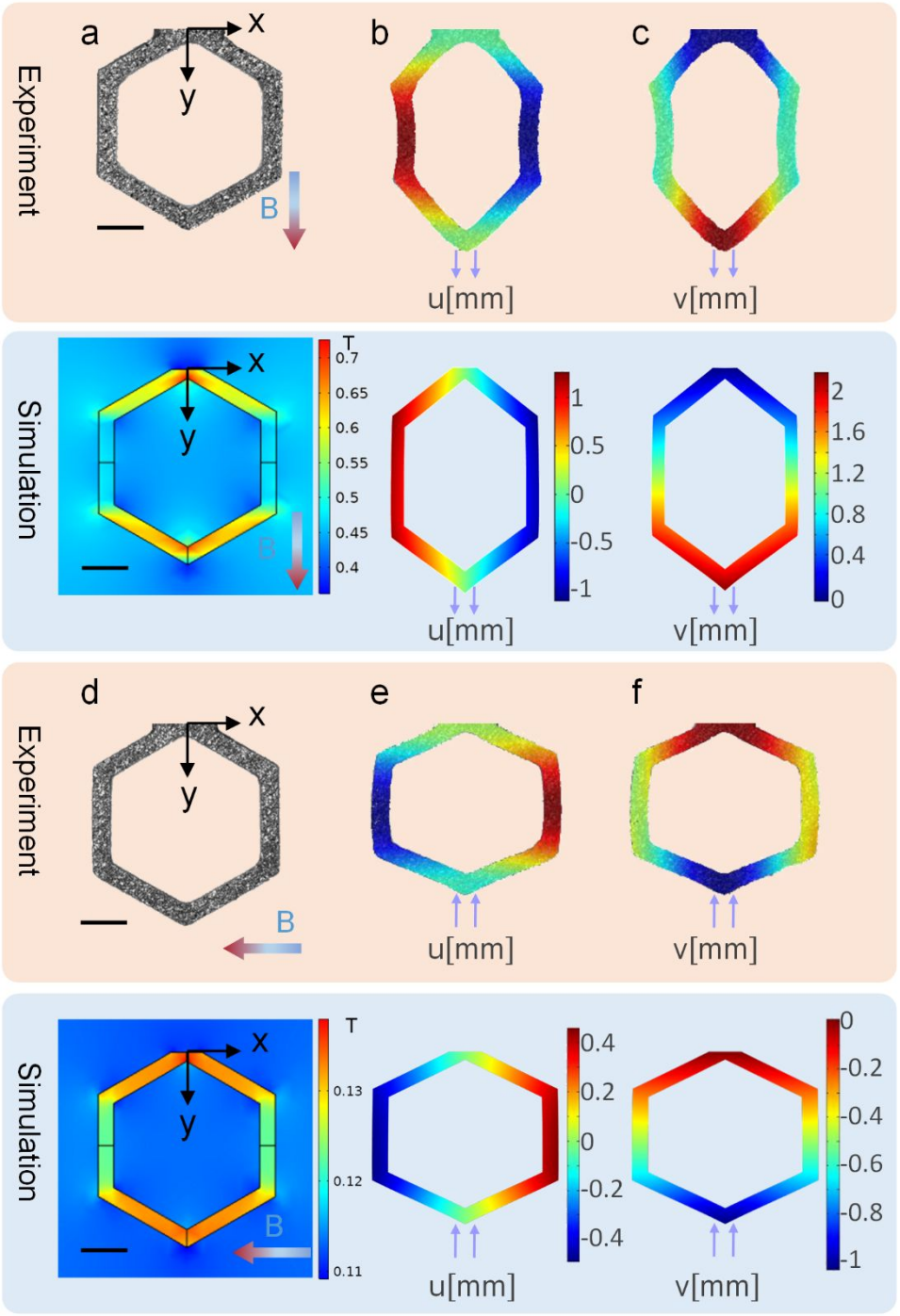

Figure S6 Magneto-deformation of regular hexagon shape anisotropic MSE. (a) The calculated magnetic flux density distribution on and around the sample under a vertical magnetic field. X-direction (b) and y-direction (c) displacement cloud images. (d-f) Results when applying a horizontal magnetic field. Scale bar, 3 mm.

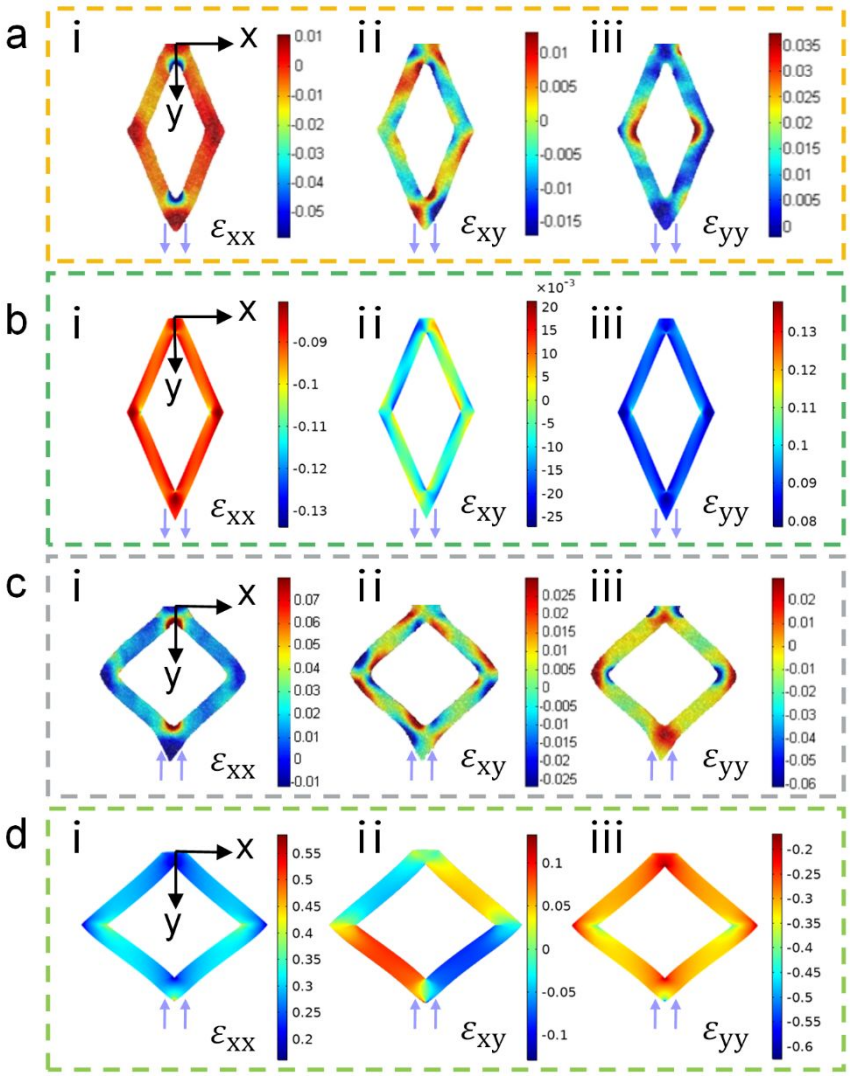

Figure S7 (a-b) Rhombic shape anisotropic MSE deforming under a vertical magnetic field, experimental and calculated strain results. (i) ε_{xx}, (ii) ε_{xy}, (iii) ε_{yy}. Experimental results (c) and simulation results (d) of strain when sample is under a horizontal magnetic field.

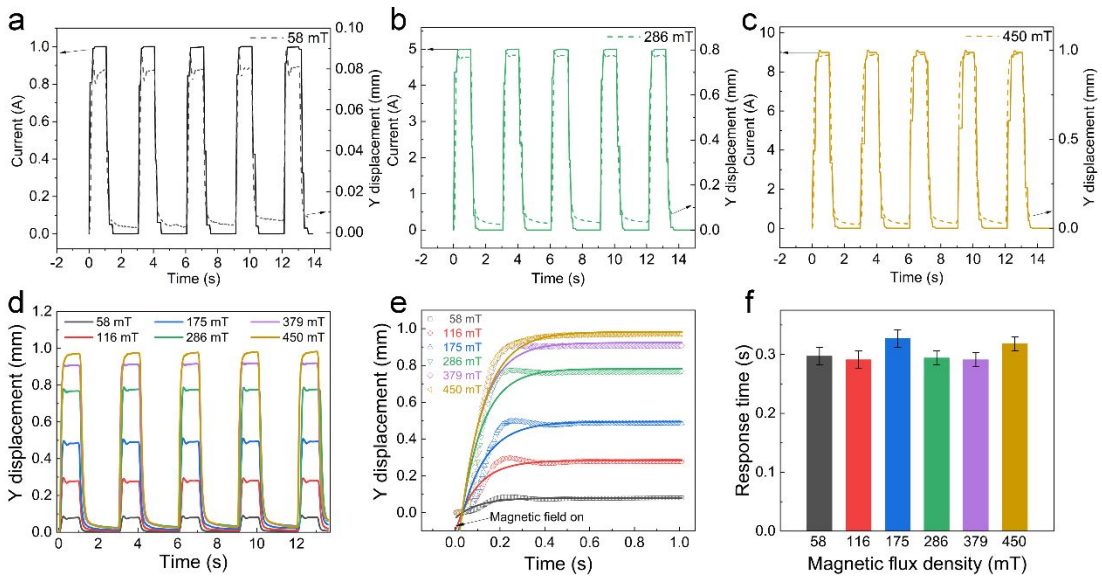

Figure S8 (a-d) The y-direction deformation response of the rhombic shape anisotropic MSE to a vertical step magnetic field with different amplitudes. (e) The y displacement with time and the fitting of experimental data (solid line). (f) The response characteristic time is calculated using the fitting parameters.

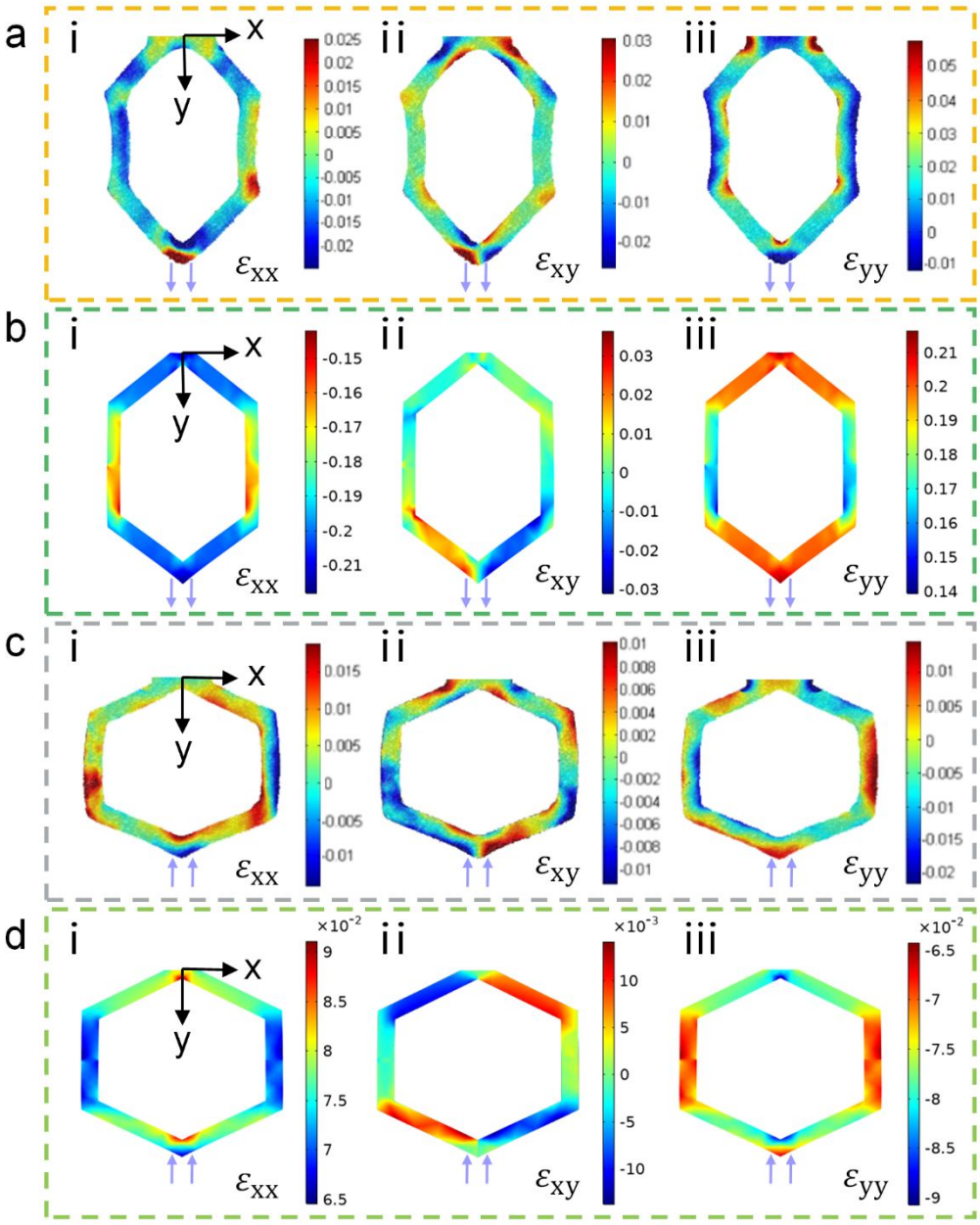

Figure S9 (a-b) Regular hexagon shape anisotropic MSE deforming under a vertical magnetic field, experimental and calculated strain results. (i) ε_{xx}, (ii) ε_{xy}, (iii) ε_{yy}. Experimental results (c) and simulation results (d) of strain when sample is under a horizontal magnetic field.

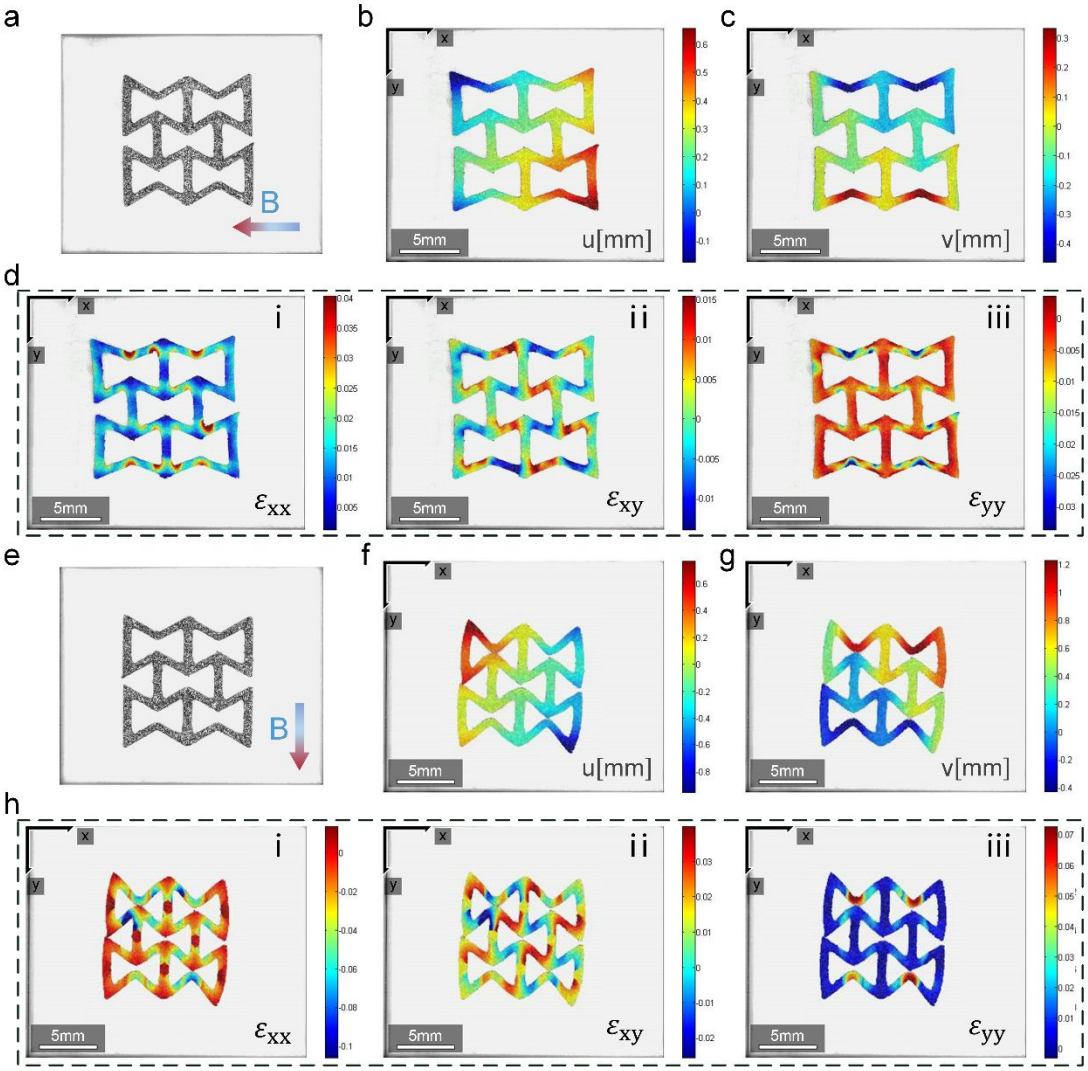

Figure S10 Displacement (b-c) and strain (d) of a re-entrant honeycomb shape anisotropic MSE (a) subjected to magnetic field. (e-h) The results of the sample under another magnetic field.

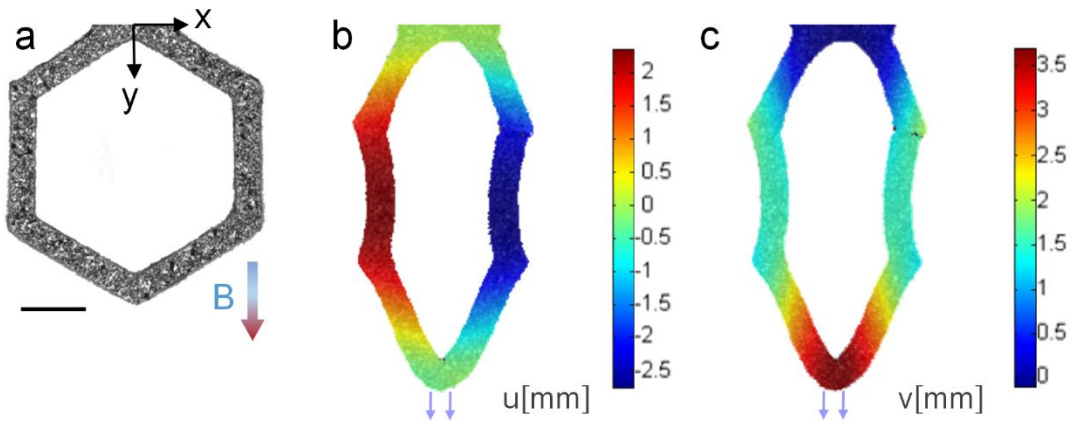

Figure S11 Regular hexagon shape material bi-anisotropic MSE (SM bi-anisotropic MSE) is subjected to a vertical magnetic field. Scale bar, 3 mm.

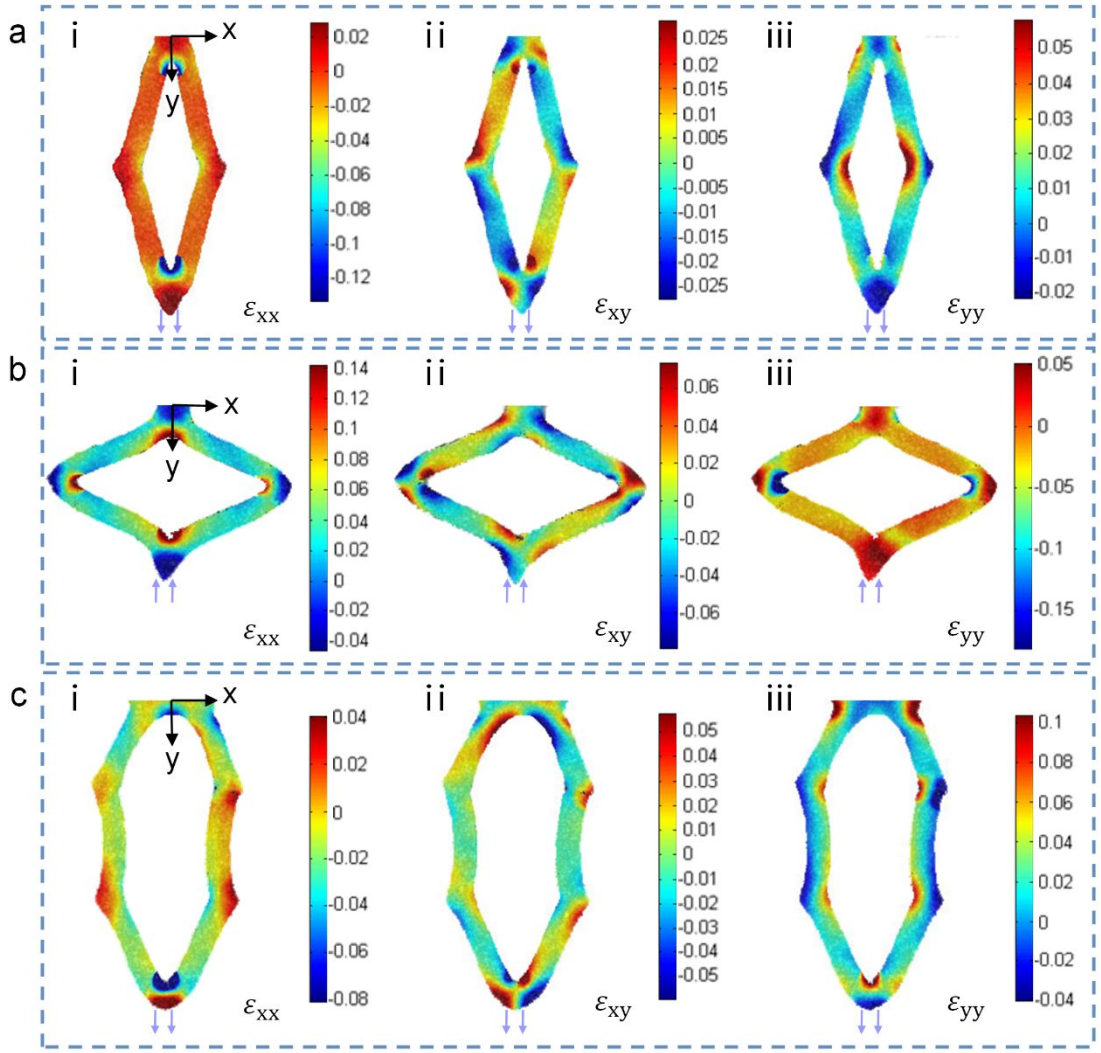

Figure S12 Strain results of rhombic SM bi-anisotropic MSE under vertical magnetic field (a), horizontal magnetic field (b) and regular hexagon SM bi-anisotropic MSE under vertical magnetic field (c).

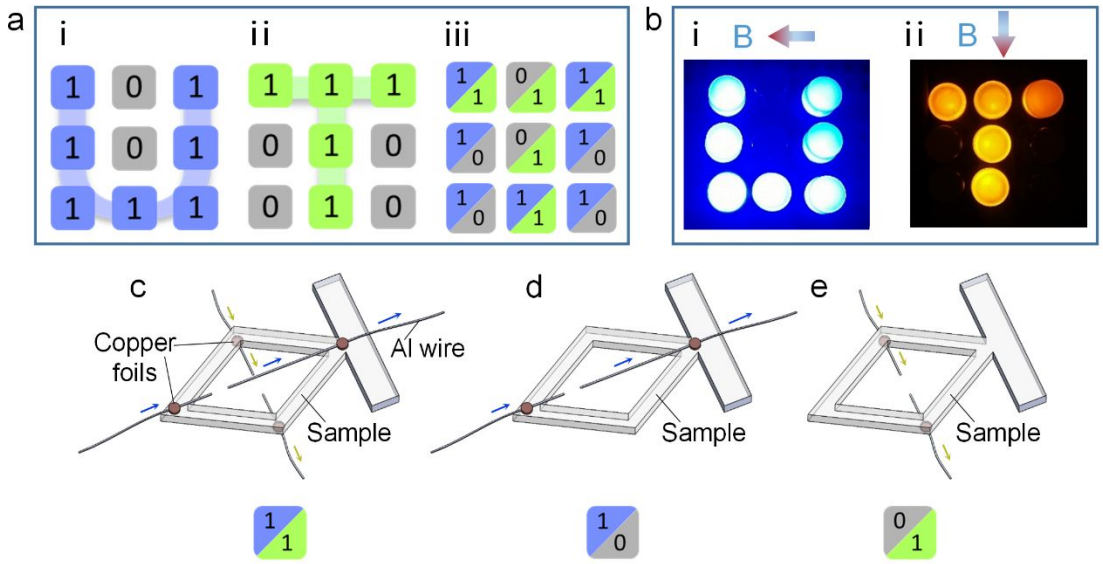

Figure S13 (a) The closed-loop is defined as 1 and open-loop is defined as 0. The letter U is programmed using a 3×3 rhombic sample switch array under a horizontal magnetic field (i). Under a vertical magnetic field, the 3×3 sample switch array programs the letter T (ii). Logical combination (iii) of (i) and (ii). (b) Under a horizontal magnetic field, the switch array lights up the letter U (i). Under a vertical magnetic field, the letter T appears (ii). (c-e) The illustrations of SM bi-anisotropic MSE based switches corresponding to the codes (1, 1), (1, 0) and (0, 1) of the alphabet switch array, respectively.

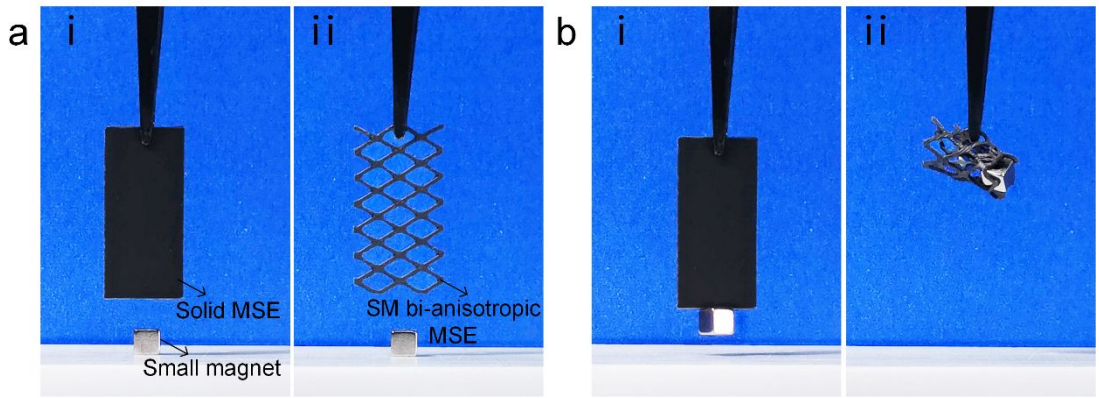

Figure S14 The comparison of solid MSE and SM bi-anisotropic MSE before (a) and after (b) trapping a magnet.

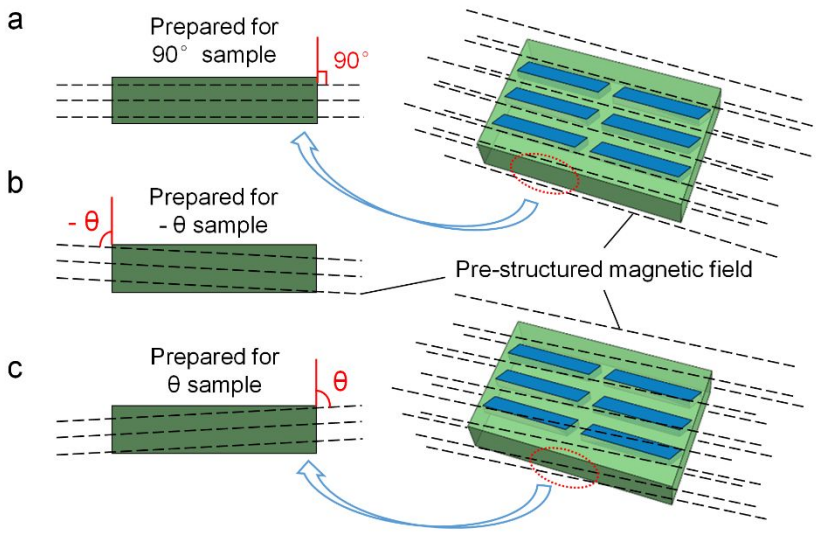

Figure S15 The pre-structured magnetic field is employed for preparing the material anisotropic 90° sample (a), the material anisotropic - θ sample (b) and θ sample (c).

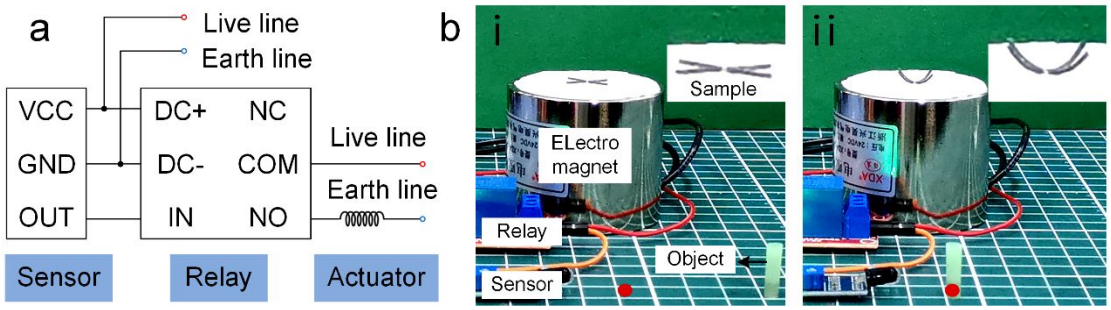

Figure S16 (a) The schematic of a multifunctional module system. (b) The sample with magnetically actuated off-plane deformation is connected with an infrared sensor to realize sentry function.

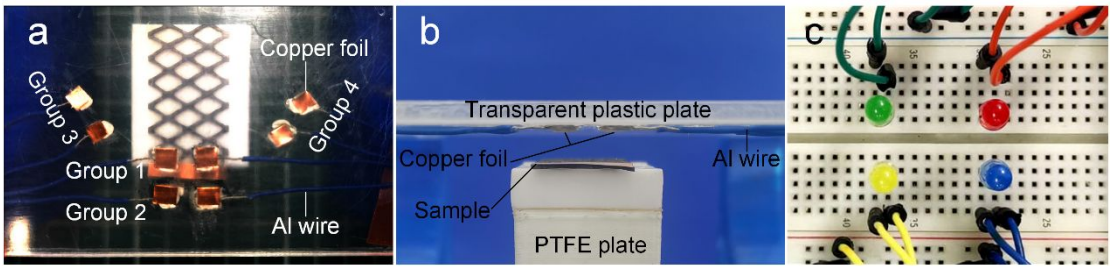

Figure S17 (a) Top view and (b) front view of the magnetic four-open switch based on a SM bi-anisotropic MSE sample. (c) The four LEDs controlled by the four groups of terminal pair.

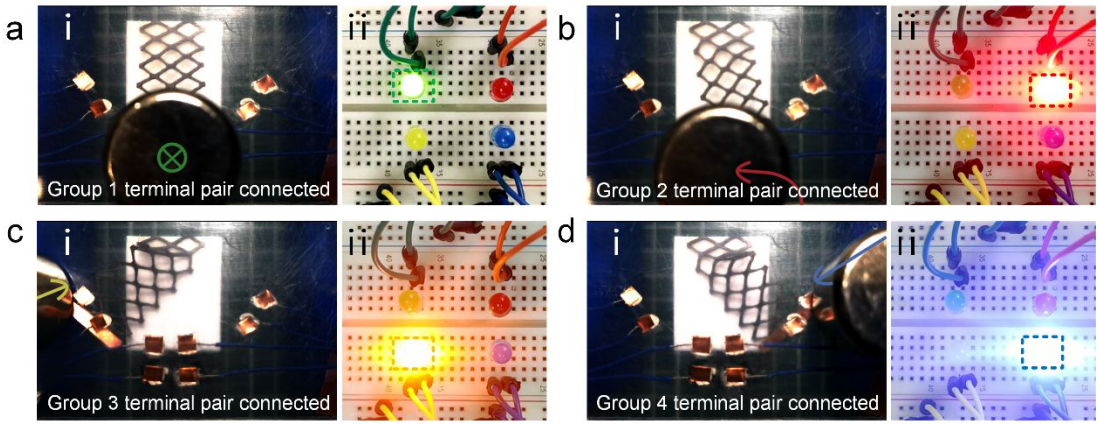

Figure S18 The effect of the magnetic four-open switch on different LEDs. The magnet reaches right above (a) or front above (b) the copper foil on the sample then the green LED or red LED lights. When the magnet approaches the third (c) or fourth (d) terminal pair along 45° direction, the sample deforms and connects the terminal pair, as a result, the yellow LED or blue LED lights.